International Journal of Architectural, Civil and Construction Sciences
ISSN: 2415-1734
Vol:12, No:11, 2018

Feasibility of Ground Alkali-Active Sandstone Powder for Use in Concrete as Mineral Admixture

Xia Chen, Hua-Quan Yang, Shi-Hua Zhou

***Abstract*—**Alkali-active sandstone aggregate was ground by vertical and ball mill into particles with residue over 45 μm less than 12%, and investigations have been launched on particles distribution and characterization of ground sandstone powder, fluidity, heat of hydration, strength as well as hydration products morphology of pastes with incorporation of ground sandstone powder. Results indicated that ground alkali-active sandstone powder with residue over 45 μm less than 8% was easily obtainable, and specific surface area was more sensitive to characterize its fineness with extension of grinding length. Incorporation of sandstone powder resulted in higher water demand and lower strength, advanced hydration of C_3A and C_2S within 3days and refined pore structure. Based on its manufacturing, characteristics and influence on properties of pastes, it was concluded that sandstone powder was a good selection for use in concrete as mineral admixture.

***Keywords*—**Concrete, mineral admixture, hydration, structure.

I. Introduction

GREAT awareness has been raised on alkali-aggregate reaction (hereafter as AAR), one of the most concerned problems hydropower station construction went great lengths to avoid [1]-[3], and preventive measures should be taken such as excavating harmful aggregates, limiting maximum alkali content in cement and concrete, adding pozzolanic materials to replace cement as well as using some inhibitor [4]-[7]. So far, hydropower stations failure caused by AAR was seldom reported in Mainland China [8], thanks to popularization of use of mineral admixture in concrete including fly ash, blast furnace slag, silica fume as well as some other pozzolanic materials [9]-[11]. Danjiangkou hydropower station, the water source of South-to-North Water Diversion project, used blast furnace slag as mineral admixture because flint was detected in aggregates. Both Xiaolangdi and Jinping I hydropower stations [7] used fly ash and low-alkali cement to batch concrete to ensure safety. So far, use of non-alkali active aggregates was the safest and most reliable measure with respect of AAR prevention, yet the selection of aggregates was subjected to many constraints considering continuous consumption of natural resources and restriction of budgets. A great challenge was approaching that active aggregates, especially silica active aggregates, were widely distributed and good quality aggregate resource was no more bottomless and inexhaustible, and when no choice was left but to use alkali active aggregates, remedial measures should be taken to ensure durability and safety of engineering structures.

So far, only seldom hydraulic engineering was reported to have used alkali active aggregates in Mainland China, in which Jinping I hydropower station construction had used marble sand and sandstone coarse aggregate to batch concrete and sandstone coarse aggregate was detected as alkali active and as aforementioned, good quality fly ash and low alkali cement were used and strict control on total amount of alkali content in concrete was implemented to ensure the safety of engineering structure. Nevertheless, so far no information on use of ground alkali-active aggregate powder in concrete as mineral admixture was reported.

This present paper had developed a new material for use in concrete as mineral admixture based on sandstone aggregate which was detected as alkali-active by accelerated mortar bar testing and supposed to be applied on a mega hydropower station construction located in southwest of China. Manufacturing and characterization of sandstone powder, fluidity, thermal and mechanical, deformation as well as durability of concrete batched with this sandstone powder were also investigated.

II. Experimental

A. Materials

Moderate heated cement (M.H.cement) with 28d compressive strength no less than 42.5 MPa was used for tests, and fly ash of good quality was also introduced for comparison tests. The chemical components of these two materials were listed in Table I and quality parameters of fly ash listed in Table II.

TABLE I
Chemical Component of Cement and Fly Ash for Tests

Type	CaO	SiO_2	Al_2O_3	Fe_2O_3	MgO	SO_3	R_2O*	Loss
M. H. Cement	59.3	22.8	3.1	4.8	4.7	2.2	0.3	1.4
Fly ash	1.8	53.0	22.9	10.2	3.3	1.0	1.5	5.6
Sandstone	2.2	64.2	14.5	5.7	4.5	0.2	3.1	3.0

Note: $Na_2O_{eq.}$ is the equivalent content of Na_2O and is calculated by $Na_2O+0.658K_2O$.

Sandstone aggregates excavated from a hydropower station construction site located in southwest of China were shifted to laboratory for tests and the aggregates were ground to powder with different fineness. The chemical components of sandstone were listed in Table I. Alkali reactivity of sandstone aggregate was detected according to ASTM C1260 and test results demonstrated in Table III, as seen, sandstone aggregate was potentially alkali active with 14d expansion exceeding 0.1% and 28d expansion reached 0.359%.

Xia Chen is with the Changjiang River Scientific Research Institute, China (e-mail: chenxia1017@126.com).

TABLE II
QUALITY PARAMETERS OF FLY ASH

Parameter	Residue over 45μm sieve (%)	Specific surface area (m^2/kg)	Water requirement ratio (%)	Apparent density (kg/m^3)	28d compressive strength ratio* (%)
Fly ash	6.6	357	101	2500	67

Note: referring to compressive strength ratio of 30%fly ash-cement mortar and controlled cement mortar

TABLE III
ALKALI REACTIVITY DETECTION OF SANDSTONE

Aggregate	Mortar bar expansion (%)				
	3d	7d	14d	21d	28d
Sandstone aggregate	0.063	0.161	0.229	0.317	0.359

Mineral determination of sandstone aggregate was launched by polarizing microscope as displayed in Fig. 1 and it was identified as the composites of siltstone rock and substrates in approximate proportion of 75:25 by mass, in which the siltstone was constituted of quartz, feldspar and biotite while substrate was composed of black organic matrix, small amount of cryptocrystalline and stripped sericite.

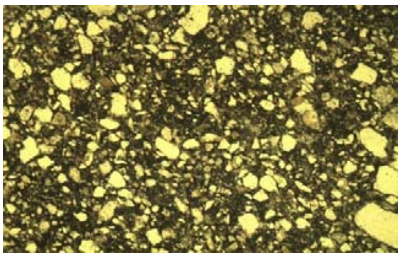

Fig. 1 Mineral determination of sandstone aggregate

B. Sampling and Test Methods

To perform fluidity and strength tests, mix proportion of mortar was prepared as cementitious materials and water ratio at 2:1 and cementitious materials and sand ratio at 3:1, and the replacement levels of supplementary materials was 15%, 25%, 35%, 45%, and 55% respectively by mass of cement, and the sandstone powder used for paste and mortar test had specific surface area of 645 m^2/kg. Superplasticizer was not used in mortar.

Heat of hydration was performed according to ASTM C186-2015 and heat releasing of composite pastes was detected by micro calorimeter C80. For heat releasing detection, 500 mg uniformly-mixed cementitious materials was prepared as sample and analytical reagent SiO_2 was used for reference, and testing temperature was controlled at 28 ℃.

Samples for compressive tests were batched with water/binder ratio of 1:2 and sand/binder ratio of 3:1.

The morphology of hydration products was observed by field scanning emission microscopy (FSEM). A comprehensive analysis of cement-ground sandstone powder paste by mercury intrusion porosimetry (MIP) technique was also performed. The low pressure of mercury intrusion ranges from 0.007 MPa to 0.207 MPa, and the high-pressure ranges from 0.207 MPa to 379.225 MPa. The measured pore sizes range from 0.003 μm to 175 μm.

III. RESULTS AND DISCUSSION

A. Manufacture of Sandstone Powder

Alkali-active sandstone aggregate was crushed by Barmac crusher into particles sized less than 10 mm which was subsequently put into vertical mill RM2200 for finer grounding. Sandstone powder particles with residue over 45 μm less than 8% was obtained by adjusting mill parameters, including segregator speeder at 40 Hz, roller pressure at 6.9 MPa, input and output temperature at 180 ℃ and 72 ℃ respectively, and the feed amount at 21t/h. The final outcome of finished powder had residue over 45 μm and 75μm at 5.8% and 0.2% respectively as displayed in Table IV, better than the set target. The morphology of ground sandstone powder was illustrated in Fig. 2.

B. Particles' Distribution and Characterization

Sandstone powder was further processed by ball mill to obtain different fineness samples. The fineness was characterized both by residue over 45 μm sieve and specific surface area, and the relationship in between was illustrated in Fig. 3. As seen, good conformity was observed between these two parameters which varied in the manner as specific surface area exhibited rising tendency as grinding length extended while residue over 45μm sieve showed decreasing trend, and when grinding length exceeded 40 minutes, specific surface area was more sensitive to characterize the fineness.

Laser particle size analyser (LPSA) produced by Beckman Coulter was employed to determine the particle size and distribution of sandstone powder as displayed in Fig. 4. Obviously, particles sized less than 80 μm accounted for over 90% by volume, in which smaller particles sized less than 16 μm ranged between 50.6% and 86.7%. As the majority of cement particles sized between 10 μm and 60 μm [12], and very large number of particles in sandstone powder sized less than 5 μm was present, and the latter could produce good filling effect among cement particles and condense the structure.

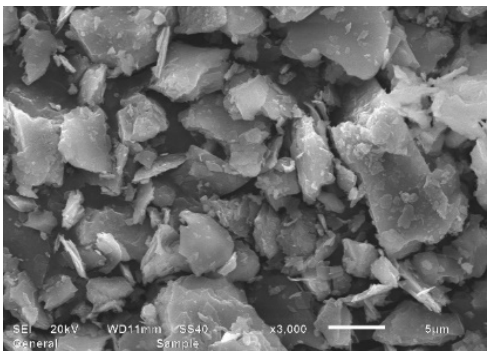

Fig. 2 Morphology of ground sandstone powder

TABLE IV
THE REAL-TIME PRODUCTION AND CHECK OF SANDSTONE POWDER

Samples	Feed amount (ton)	Segregator speed (Hz)	Mill pressure (MPa)	Input temperature (℃)	Output temperature (℃)	Fineness (%) residue over 45μm	Fineness (%) residue over 75μm
1	30	40	7.20	184	76	4.7	0.1
2	32	36	6.82	188	73	6.0	0.2
3	32	36	7.70	191	75	6.2	0.1
4	32	36	6.94	189	76	5.8	0.2
5	32	36	6.79	182	77	6.5	0.2
Average	32	36	7.00	185	70	5.8	0.2

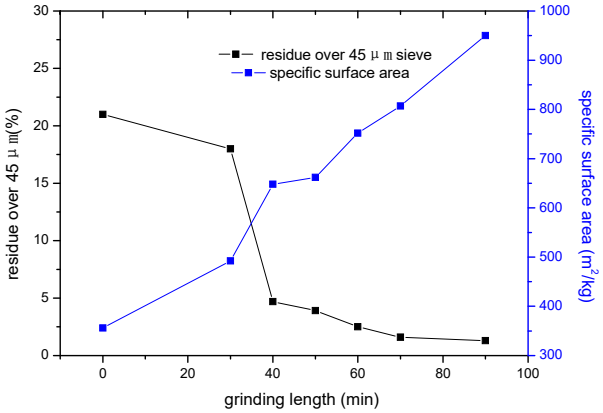

Fig. 3 Specific surface area vs. residue over 45 μm sieve

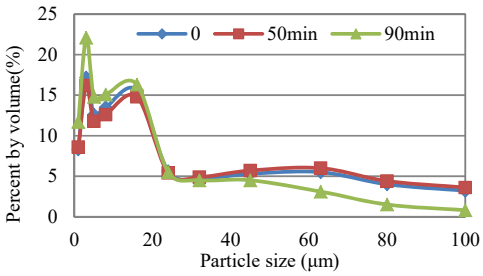

(a) Particles size and distribution

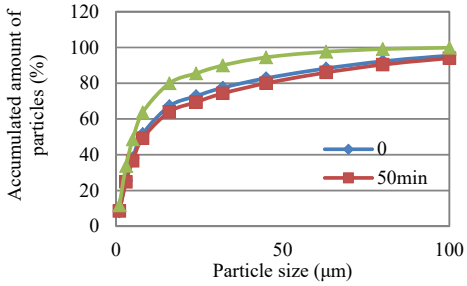

(b) Accumulative percent

Fig. 4 Particles characteristics of sandstone powder of different fineness

C. Fluidity of Composite Pastes

Sandstone powder was incorporated in paste replacing cement in different proportions ranging from 15% to 55% and its influence on fluidity of pastes was illustrated in Fig. 5, also comparison with fly ash was conducted. Obviously, sandstone powder had adverse effect on fluidity of pastes, which varied in the manner as fluidity decreased with increment in sandstone powder content ranging between 15% and 55%, while the trend was reversed with respect to fly ash paste. The results implied that sandstone powder in use of concrete as mine admixture would result in higher unit water demand and in order to maintain the same fluidity larger amount of water reducer was required in case of the same mix proportion.

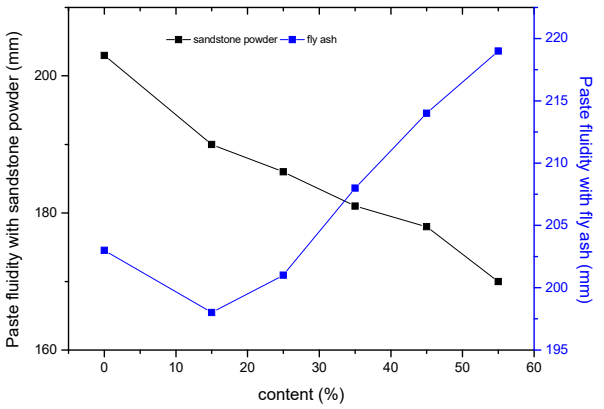

Fig. 5 Fluidity of composite pastes with incorporation of sandstone powder and fly ash

D. Heat of Hydration

The heat of hydration of composite pastes with incorporation of sandstone powder and fly ash respectively was tested according to ASTM C186-2015, and results were illustrated in Fig. 6, and heat releasing of composite pastes was also detected with introduction of micro calorimeter as demonstrated in Figs. 7 and 8, in which the characterized values of heat flow of hydration released by composite paste were listed in Table 5.

As clearly seen, the heat of hydration of composite pasts was lower than the control mixture despite of different replacements and the reduction magnitude grew more obvious as increase in content of supplementary materials. In case of the same supplementary content, ground sandstone powder-cement pastes produced a little higher heat of hydration than fly ash-cement pastes within 7d testing age, which was interpreted as micro particles with greater specific surface area in ground sandstone powder had accelerated hydration of cement clinker [14] and part of sandstone powder participated in hydration.

The hydration process of composite pastes was also grouped into five stages according to Figs. 7 and 8 and incorporation of sandstone powder reduced total heat of hydration within 72h by 15% which was exactly the content of sandstone powder replacing cement by mass, in good conformity with aforementioned strength decreasing magnitude.

By comparison of heat flow peaks in Table 5, sandstone powder had advanced hydration of C3A from 276.8 s to 224.9 s and decreased heat flow only by 5%, lower than its replacement of 15%. Accordingly, heat flow peak produced by hydration of C2S and C3S was advanced from 9.45h to 8.91h and its heat flow peak reduced by 9%, also lower than the replacement of sandstone powder. The results implied that sandstone powder had accelerated larger amount of cement clinker participating in hydration within 3d and some of sandstone powder also had hydrated under alkali environment and made its contribution to heat of hydration.

E. Compressive Strength of Composite Pastes

Fig. 9 presents the compressive strength of composite pastes with sandstone powder (specific surface area of 645 m^2/kg) and fly ash incorporated respectively. The compressive strength of all composite pastes was lower than the control mixture in spite of ages and replacement ratio, whereas significant increase in compressive strength of composite paste with sandstone powder was observed when testing age was extended from 3d to 28d, while it was slowed down from 28d to 90d. Obviously, fly ash pastes produced greater compressive strength increase than sandstone powder pastes with testing age extending when replacement by mass of cement was less than 45%, which justified higher pozzolanic reactivity of fly ash and greater contribution to strength gain produced by reacting with $Ca(OH)_2$ released from hydration of cement [13].

TABLE V
CHARACTERIZED VALUES OF HEAT FLOW OF HYDRATION RELEASED BY CEMENT-BASED MATERIALS

Cementitious System	Total heat of hydration	Heat flow peak at pre-induction stage		Heat flow peak at accelerating stage	
	kJ/kg	Occuring time/s	Heat flow/mW	Occuring time/h	Heat flow/mW
Cement	198.0/100%	276.8	1.402/100%	9.45	1.155/100%
15%sandstone powder-cement	168.4/85%	224.9	1.331/95%	8.91	1.056/91%

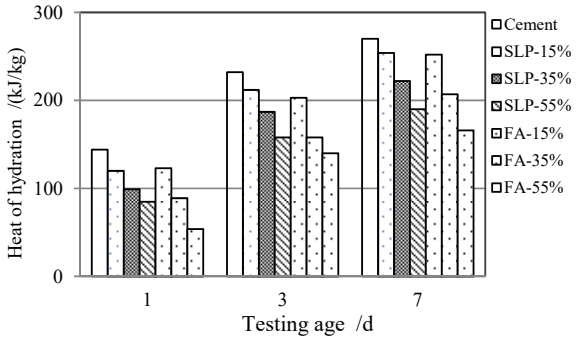

Fig. 6 Heat of hydration of composite pastes

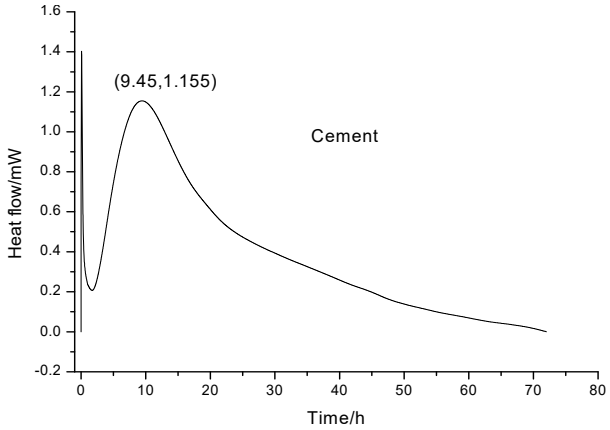

(a) 72h

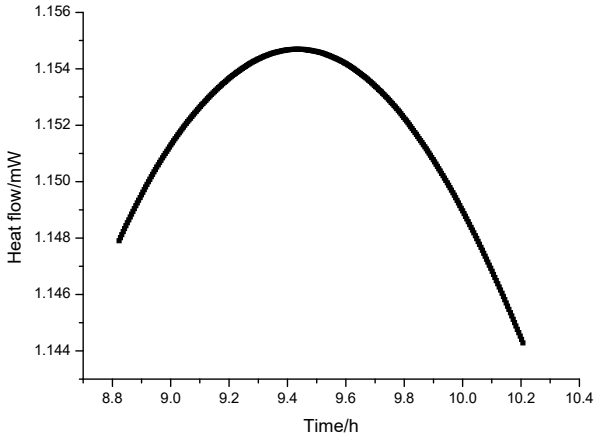

(b) II heat peak

Fig. 7 Heat releasing of cement paste

F. Pore Structure of Composite Pastes

Pore structure of composite pastes was illustrated in Table 6 and Fig. 10. Porosity of composite pastes exhibited decreasing tendency with development of curing time while showed a rising trend with increase in replacement of sandstone by mass of cement. Besides, when the replacement of sandstone powder increased from 25% to 35%, the per cent of pores sized less than 100 nm which was believed to have positive effect on various performances of pastes had also decreased from 66.22% to 57.71% at 28d.

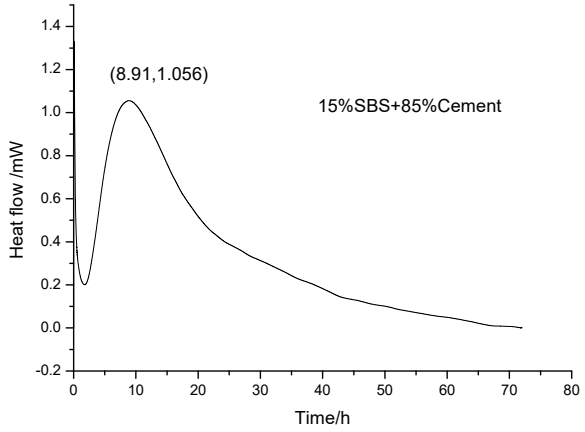

(a) 72h

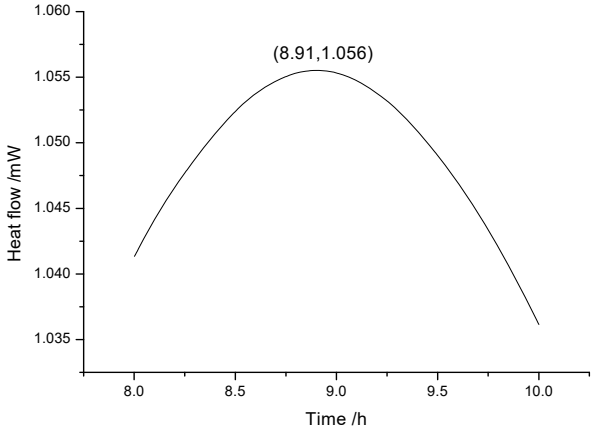

(b) II heat peak

Fig. 8 Heat releasing of 15% sandstone powder-cement paste

At replacement of 35%, the porosity of sandstone powder composite paste decreased from 23.01% at 3d to 19.63% at 28d, and the percent of pores sized less than 100 nm had correspondingly increased from 26.14% to 57.71%. By comparison, combination of fly ash and sandstone powder with replacement of 25% in total had no obvious effect on early pore structures, in good conformity with aforementioned strength development from 7d to 28d, yet good improvement was observed from 7d to 180d with porosity decreasing from 19.20% to 13.04% and percent of pores less than 50 nm increasing from 28.96% to 48.08% dramatically.

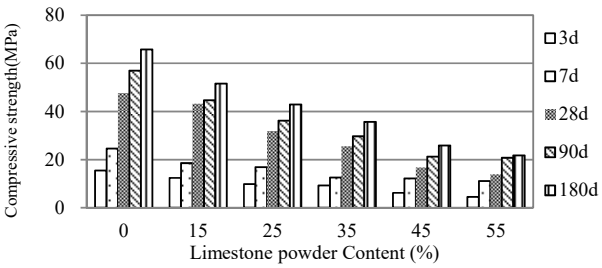

(a) Replacement of 0~55% of cementitious materials by sandstone powder

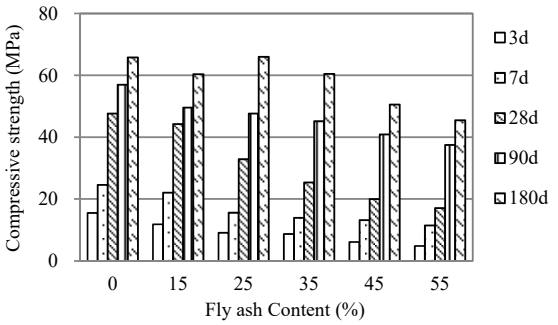

(b) Replacement of 0~55% of cementitious materials by fly ash

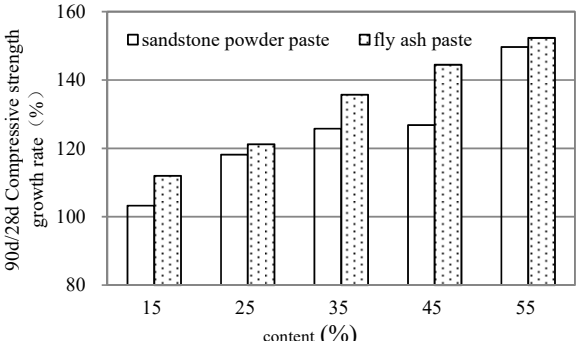

(c) 90d/28d ratio

Fig. 9 Compressive strength of composite pastes

TABLE VI
POROSITY AND PORES DISTRIBUTION OF PASTES

No.	SCM	Age (d)	Porosity (%)	Pore distribution (nm)			
				<5	5~50	50~100	100~200
SBS-25%	25%sandstone powder	7	19.20	4.56	24.61	11.17	59.66
		28	17.83	7.82	36.92	21.48	33.78
SBS-35%	35% sandstone powder	3	23.01	1.95	16.68	7.51	73.86
		7	21.70	2.64	20.51	8.65	68.20
		28	19.63	5.71	32.78	19.22	42.29
SBF	15%SBS+10%FA	3	21.17	2.24	17.12	8.38	72.26
		7	19.20	4.32	24.64	10.99	60.05
		180	13.04	8.31	39.77	9.32	42.60

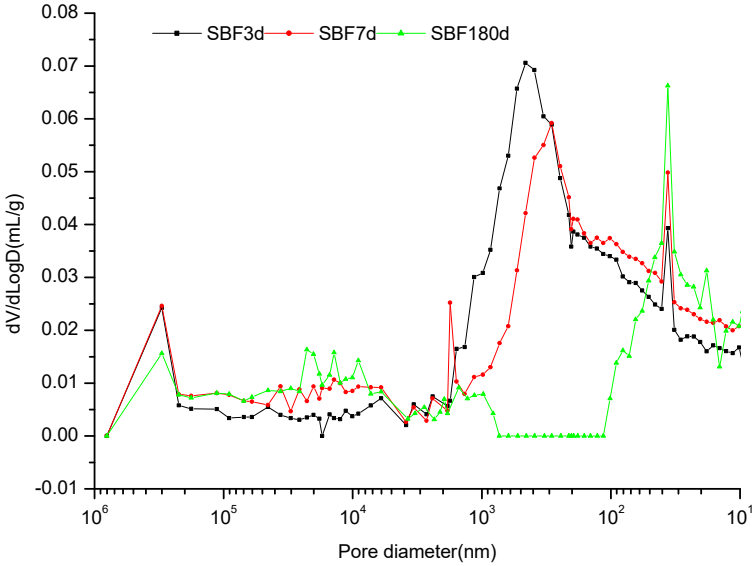

(a) Sandstone powder and fly ash

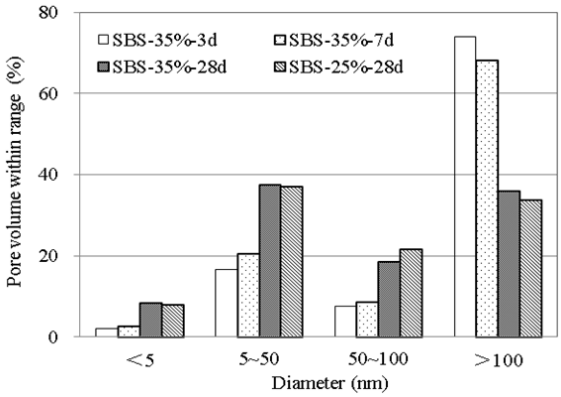

(b) Sandstone powder

Fig. 10 Porosity and pores distribution of composite pastes

G. Hydration Products Morphology

Fig. 11 presented the morphology of products of hydration of composite pastes at different ages, and the products of hydration were primarily consisted of lathy and fibre C-S-H, flaked and granules crystalline, which grew outside from the surface of un-hydrated particles, and many products of hydration was discernible from the pastes and no big difference was observed in the total amount of products of hydration between composite pastes adding fly ash and sandstone powder respectively at the same age. At 28d, the produced C-S-H gel of fly ash pastes sized between 5 μm and 10 μm and part of products of hydration covered on the surface of fly ash particles, and the structure grew more tense with age despite of visible voids. As for the sandstone powder-fly ash-cement ternary composite, large amount of products of hydration was also distinguished from Fig. 10 and C-S-H gel had length of approximately 5 μm~10 μm, and by 180d the ternary composite structure grew condense and fly ash particle was fiercely beset by products of hydration.

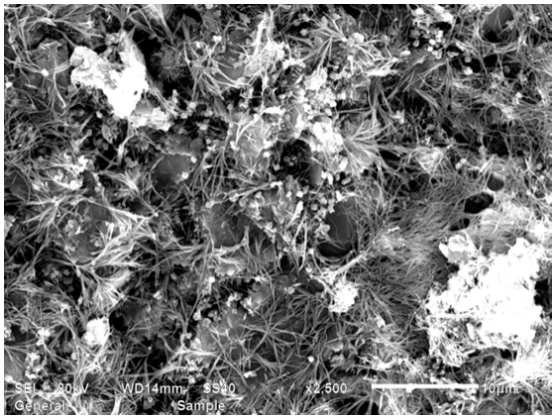

(a) 25% sandstone powder-28d

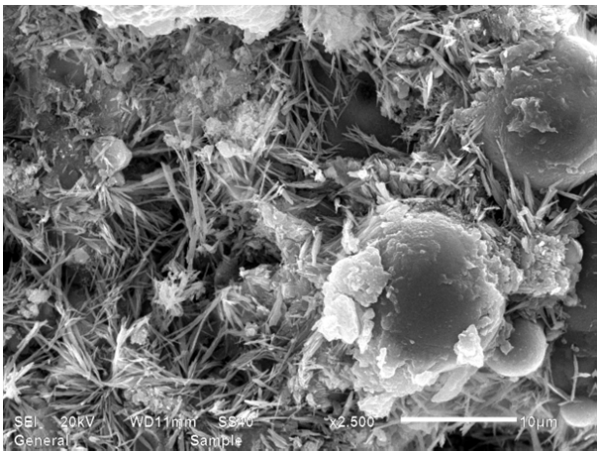

(b) 25% fly ash-28d

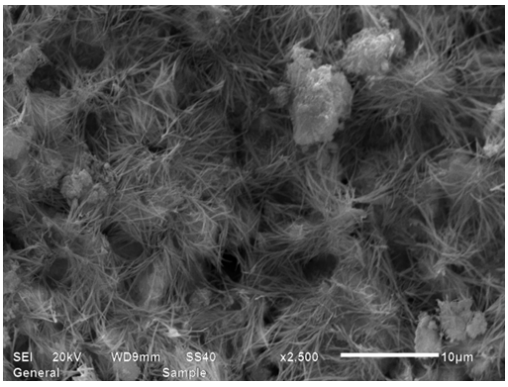

(c) 15% sandstone powder+10%fly ash-3d

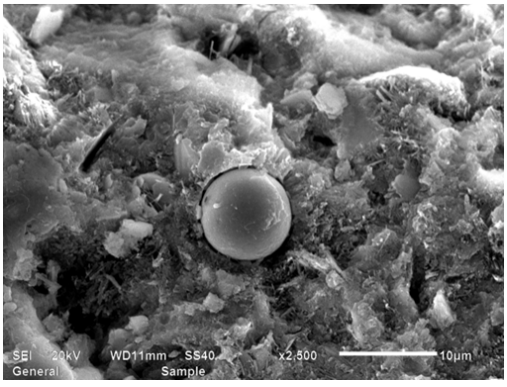

(d) 15% sandstone powder+10%fly ash-180d

Fig. 11 SEM patterns of composite pastes

IV. Conclusions

Hydration characteristics and microstructure of composite system was reached that ground alkali-active sandstone powder was feasible for use in concrete as mineral admixture. Ground alkali-active sandstone powder with residue over 45 μm less than 8% was easily obtainable by vertical and ball mill, and incorporation of sandstone powder would increase unit water demand and decrease early strength of composite pastes, yet it also advanced hydration of C_3A and C_2S within 3days and refined pore structure.

Acknowledgment

The financial help of Yalong River Hydropower Development Co.Ltd, National Key Technology Research and Development Program of China (Project No. 2016YFB0303601) and the National Natural Science Foundation of China (Project No. 51479011 and No.51409016) are gratefully acknowledged.

References

[1] Tang M S. Review on AAR development over the world. China Concrete and Cement Products, 1993, 1:4-6.
[2] Shi, C, Shi, Z, Hu, X, et al. A review on alkali-aggregate reactions in alkali-activated mortars/concretes made with alkali-reactive aggregates. Materials and Structure, 2015, 48(3): 621-628.
[3] Costa, F L, Torres, A S& Neves, R.A. J. Analysis of concrete structures deteriorated by alkali-aggregate reaction: case study. Journal of Building Pathology and Rehabilitation, 2016, 1: 13.
[4] Mohamed, I, Curtil, L, Ronel-Idrissi, S. et al. Influence of composite materials confinement on alkali aggregate expansion. Materials and Structure, 2005, 38(3): 387-394.
[5] Mo, I. X. Y., Xu, Z. Z., Wu, K. R. et al. Effectiveness of LiOH in inhibiting alkali-aggregate reaction and its mechanism(J). Materials and Structure, 2005, 38(1): 57-61.
[6] Li P X, Wang L, Peng S S. Experimental study on measures for inhibiting alkali - aggregate reaction of quartz sandstone. Yangtze River, 2013,7:75-78.
[7] Li G W, Zhou Q W. Engineering measures for inhibiting concrete alkali-aggregate response during construction of high arch dam of Jinping I Hydropower Station. Water Resources and Hydropower Engineering, 2013, 1:45-49.
[8] Li J Y. Alkali-aggregat reaction in dam concrete of China.Water Power, 2005, 1:34-37.
[9] Yang H Q, Li P X, Chen X. The State-of-art of Alkali Aggregate Reaction of Hydraulic Concrete. Journal of Yangtze River Scientific Research Institute, 2014, 10:58-62.
[10] Yang H Q, Li P X. Experimental study on alkali-reactive granitic aggregates of Three Gorges project. Journal of Hydroelectric Engineering, 2010, 2:222-227.
[11] Dong Y, Yang H Q, Li P X. Research on inhibition of alkali aggregate reactivity with natural pozzolans. Concrete, 2011, 11:77-79.
[12] Zhu B L, Huang X, Guo Ye, e tal. Packing Density of Cement in Paste with Continuous Grain Size Distribution. Journal of Building Materials, 2006, 4:447-452.
[13] Wang C, Yang C H, Qian J S, e tal. Behavior and Mechanism of Pozzolanic Reaction Heat of Fly Ash and Ground Granulated Blastfurnace Slag at Early Age. Journal of The Chinese Ceramic Society, 2012, 7:1050-1058.
[14] Song J W, Wang L, Liu S H, et al. Functionary Mechanism of Limestone Powder in Ultra High Performance Cement-Based Materials. Bulletin of the Chinese Ceramic Society, 2016, 4:4104-4109.